



**HAL**  
open science

## Observation potential of the decays $B^0_{s,d} \rightarrow J/\psi\eta$ in the ATLAS experiment at the LHC

C. Driouichi, P. Eerola, M. Melcher, F. Ohlsson-Malek, S. Viret

► **To cite this version:**

C. Driouichi, P. Eerola, M. Melcher, F. Ohlsson-Malek, S. Viret. Observation potential of the decays  $B^0_{s,d} \rightarrow J/\psi\eta$  in the ATLAS experiment at the LHC. EPJdirectC - Scientific notes, 2002, 4, pp.1-13. 10.1007/s1010502cn002 . in2p3-00011351

**HAL Id: in2p3-00011351**

**<https://hal.in2p3.fr/in2p3-00011351>**

Submitted on 28 Mar 2002

**HAL** is a multi-disciplinary open access archive for the deposit and dissemination of scientific research documents, whether they are published or not. The documents may come from teaching and research institutions in France or abroad, or from public or private research centers.

L'archive ouverte pluridisciplinaire **HAL**, est destinée au dépôt et à la diffusion de documents scientifiques de niveau recherche, publiés ou non, émanant des établissements d'enseignement et de recherche français ou étrangers, des laboratoires publics ou privés.

ISN-01.68  
LUNFD6/(NFFL-7198) 2001  
SN-ATLAS-2002-011  
March 8<sup>th</sup>, 2002.

## Observation potential of the decays $B_{s,d}^0 \rightarrow J/\psi\eta$ in the ATLAS experiment at the LHC

C. Driouichi<sup>a</sup>, P. Eerola<sup>a</sup>, M. Melcher<sup>b</sup>, F. Ohlsson-Malek<sup>b</sup>, S. Viret<sup>b</sup>

<sup>a</sup> Department of Elementary Particle Physics, Lund University,  
Box 118, S-221 00 Lund, Sweden

<sup>b</sup> Institut des Sciences Nucléaires, Université J. Fourier,  
IN2P3-CNRS, F-38026 Grenoble, France

### Abstract

The observation potential of the decays  $B_{s,d}^0 \rightarrow J/\psi\eta$  with the ATLAS detector at the LHC is described in this paper. At present there exist only upper limits for the branching fractions, but at LHC, a clear signal for the decay mode  $B_s^0 \rightarrow J/\psi\eta$  is expected. The branching fraction of this decay mode can thus be measured, and other parameters such as  $B_s^0$  lifetime can be measured as well.

The decay mode  $B_s^0 \rightarrow J/\psi\eta$  is analogous to the mode  $B_s^0 \rightarrow J/\psi\phi$ , which has been studied extensively in view of CP violation measurements. In these two decay modes, the CP asymmetry predicted by the Standard Model is very small, and the observation of a sizeable effect would be a signal of physics beyond the Standard Model. The decay mode  $J/\psi\eta$  constitutes thus a cross-check for the mode  $J/\psi\phi$ . Furthermore, the former final state is a CP-eigenstate and no angular analysis is thus needed.

The reconstruction of  $\eta$ -mesons at LHC experiments has not been addressed before, and therefore the study presented here can also be regarded as an example of the physics prospects with  $\eta$ -mesons at the LHC.

## 1 Introduction

The decay  $B_s^0 \rightarrow J/\psi\eta$  can be used to measure various parameters in the  $B_s^0$ -meson system. Compared to the analogous decay mode  $B_s^0 \rightarrow J/\psi\phi$ , the advantage of this decay mode is that it is a CP eigenstate. CP eigenstates in the decay mode  $B_s^0 \rightarrow J/\psi\phi$  can be separated by means of an angular analysis of the final state, but the a priori unknown strong phases between the eigenstates are extra free parameters in the analysis which have to be sorted out.

At present the upper limit for the branching fraction for  $B_s^0 \rightarrow J/\psi\eta$  is  $3.8 \cdot 10^{-3}$  at 90% CL [1, 2]. The estimate for the branching fraction is  $(8.3-9.5) \cdot 10^{-4}$  [3], where the uncertainty is coming from uncertainty in the  $\eta - \eta'$  mixing angle. In the ATLAS experiment, assuming an integrated luminosity of  $30 \text{ fb}^{-1}$  corresponding to the first years of the LHC operation at the initial luminosity of  $(1-2) \cdot 10^{33} \text{ cm}^{-2} \text{ s}^{-1}$ , roughly 10 000 decays can be reconstructed as shown later in this paper, with a signal-to-background ratio of about 1:1. It can be thus foreseen that the following measurements will be feasible :

- measurement of the branching fraction  $B_s^0 \rightarrow J/\psi\eta$ ,
- measurement of the  $B_s^0$  lifetime.

The lifetime will be measured with other decay channels as well, so the measurement performed with the  $J/\psi\eta$  constitutes an important cross-check. Eventually, a high-statistics measurement of the  $B_s^0 \rightarrow J/\psi\eta$  branching ratio could allow imposing constraints on the  $\eta - \eta'$  mixing angle.

The CP asymmetry in the decays with quark-level transitions  $\bar{b} \rightarrow \bar{c}c\bar{s}$ , including decays  $B_s^0 \rightarrow J/\psi\phi$ ,  $B_s^0 \rightarrow J/\psi\eta^{(\prime)}$  and  $B_s^0 \rightarrow D_s^+ D_s^-$ , is predicted to be very small in the Standard Model. The time-dependent CP asymmetry for  $B_s^0$  decay into a final CP eigenstate  $f$  is :

$$a_{CP}(t) = \frac{\Gamma(B_s^0(t) \rightarrow f) - \Gamma(\bar{B}_s^0(t) \rightarrow f)}{\Gamma(B_s^0(t) \rightarrow f) + \Gamma(\bar{B}_s^0(t) \rightarrow f)} \\ \propto \sin \phi_M \sin \Delta m_s t$$

where

$$\phi_M = -2\lambda^2\eta = -2\lambda \sin \gamma |V_{ub}|/|V_{cb}|,$$

where  $\lambda = \sin \theta_C$ ,  $\theta_C$  is the Cabibbo angle,  $\eta$  is the height of the Unitarity Triangle and  $\gamma$  is one of the angles of the Unitarity Triangle. The value of  $\phi_M$  is expected to be 0.024–0.054, the Standard Model preferred value being 0.039 [4], and therefore, the extraction of the angle  $\gamma$  from the  $\phi_M$  measurement is difficult. On the other hand, these decays are sensitive to processes

beyond the Standard Model which typically increase the asymmetry. For example, in a left-right symmetric model with spontaneous CP violation [5], the CP asymmetry may be as large as  $\mathcal{O}(40)\%$ , while the model predicts for the ‘golden decay mode’  $B_d^0 \rightarrow J/\psi K_S^0$  a 10% CP asymmetry.

It has been proposed that the angle  $\gamma$  of the Unitarity Triangle could be extracted from measurements of the decay rates of  $B_s^0$  and  $B_d^0$  to  $J/\psi\eta$  [3]. While the phase  $\exp(i\gamma)$  is CKM suppressed for the decay mode  $B_s^0 \rightarrow J/\psi\eta$ , this is not the case for the decay mode  $B_d^0 \rightarrow J/\psi\eta$ . CP violation effects could thus potentially be more easily accessible through the latter mode by measuring the time-dependent asymmetry of  $B_d^0$ . The overall normalization can be fixed by measuring CP averaged rates of  $B_d^0 \rightarrow J/\psi\eta$  and  $B_s^0 \rightarrow J/\psi\eta$ , which assumes the validity of the U-spin symmetry (the approximate symmetry of u, d and s quarks). The measurements seem to be, however, out of reach due to the small expected branching ratio of  $B_d^0 \rightarrow J/\psi\eta$ , and the overlapping mass peaks of the  $B_s^0$  and  $B_d^0$ .

The paper is organized as follows. In section 2 the simulation and analysis procedures for ATLAS are described. The results are presented in section 3: event rates and prospects for CP asymmetry and angle  $\gamma$  measurements. In section 4 some comparisons with other experiments are presented, and section 5 summarises the paper.

## 2 Event reconstruction

### 2.1 Event generation and simulation

The decays  $B_{s,d}^0 \rightarrow J/\psi\eta$  were implemented in the Monte Carlo program PYTHIA 5.7 [6] in order to generate the signal sample. In the event generation, b-quark pairs were produced in pp-collisions at  $\sqrt{s} = 14$  TeV either directly via the lowest order process, or via gluon splitting or flavour excitation.

Events containing a  $B_{s,d}^0$  meson were selected, and then the  $B_{s,d}^0$  was forced to decay into a  $J/\psi\eta$  final state. The  $J/\psi$  meson was forced to decay into  $\mu^+\mu^-$ , and only events passing the ATLAS level-1 trigger requirements for B hadrons (a muon with a  $p_T > 6$  GeV and  $|\eta| < 2.4$ )<sup>1</sup> and the  $\eta$  meson decaying into  $\gamma\gamma$  were retained. The branching ratio for the decay  $\eta \rightarrow \gamma\gamma$  is  $(39.33 \pm 0.25)\%$ [1]. Events were further selected to satisfy the ATLAS second level trigger: the presence of a second muon with  $p_T > 3$  GeV and  $|\eta| < 2.5$ . The resulting signal samples were consisting of about 17 000  $B_s^0$  events and 15 000  $B_d^0$  events.

Other decay modes of the  $\eta$  meson with large branching fractions are the decays  $\eta \rightarrow 3\pi^0$  (BR= $(32.24 \pm 0.29)\%$ ) and  $\eta \rightarrow \pi^+\pi^-\pi^0$  (BR= $(23.0 \pm$

---

<sup>1</sup>Throughout this paper, the symbol  $p_T$  is used for the transverse momentum with respect to the beam direction, and  $\eta$  for the pseudorapidity.

0.4) %) [1]. While the reconstruction of the former decay is not feasible in the ATLAS experiment, the latter decay mode could potentially be used for increasing the statistics. In this paper, however, we concentrate on the two-photon decay mode of the  $\eta$  meson.

The background considered was a sample of  $B \rightarrow J/\psi X$  decays, processed and selected in the same way as the signal events. The background from fake  $J/\psi$ 's is estimated to be small when reconstructing B-mesons including  $J/\psi$ 's, and the background from primary  $J/\psi$ 's has been shown to be small when applying a cut on the decay vertex of the  $J/\psi$  [7].

A full GEANT-based simulation was used to simulate the response of the ATLAS inner detector and the electromagnetic calorimeter. The muon chambers were not included in the simulation, but only real muons were included in the analysis. The muon identification efficiencies were assumed to be 85% for the first muon (the muon with  $p_T > 6$  GeV) and 78% for the second muon (the muon with  $p_T > 3$  GeV). The 85% efficiency for the muon with the higher transverse momentum includes both reconstruction and level-1 trigger efficiencies.

The muon reconstruction efficiencies were estimated as follows. The ATLAS muon spectrometer reaches its full efficiency when the muon transverse momentum is about 6 GeV. In Ref. [8], the muon reconstruction efficiency in b-jets was found to be about 90% for muons with  $p_T > 6$  GeV. The fraction of fake muons in these jets was found to be 0.5% or less. The muons were reconstructed by combining the muon chamber and the inner detector data.

Below  $p_T = 6$  GeV, the muon identification efficiency decreases with decreasing transverse momentum. The muon reconstruction efficiencies and fractions of fake muons in the transverse momentum range  $3 \text{ GeV} < p_T < 6 \text{ GeV}$  were found to be in Ref. [8] 20% (0.1%), 37% (0.2%) and 70% (0.5%) at  $p_T = 3, 4, 5$  GeV, respectively, combining the muon chamber and the inner detector data.

For muons with  $2 \text{ GeV} < p_T < 6 \text{ GeV}$ , the ATLAS tile calorimeter can be used to aid the muon identification in the barrel region ( $|\eta| < 1.75$ ). In Ref. [8], the muon reconstruction efficiency in the tile calorimeter was found to be 75%. The hadron rejection factor was about 10. Combining the muon chamber and the tile calorimeter muon identification, the efficiencies would thus be 80%, 84% and 93% in the barrel ( $|\eta| < 1.75$ ) and 20%, 37% and 70% in the end-caps ( $1.75 < |\eta| < 2.5$ ) at  $p_T = 3, 4, 5$  GeV, respectively.

Folding these reconstruction efficiencies with the transverse momentum and pseudorapidity distribution of the second muon (the muon with a  $p_T > 3$  GeV,  $|\eta| < 2.5$ ), the average efficiency was found to be 78%. The first muon (the muon with a  $p_T > 6$  GeV,  $|\eta| < 2.4$ ) reconstruction efficiency was 90%, but the overall efficiency was set to 85% to take into account the level-1 trigger efficiency.

Electronic noise and pile-up corresponding to  $\mathcal{L} = 10^{33} \text{ cm}^{-2} \text{ s}^{-1}$  were added to the electromagnetic calorimeter raw data at the reconstruction

level as described in Ref. [9].

## 2.2 Reconstruction of $B_{s,d}^0 \rightarrow J/\psi\eta$

The  $J/\psi$  was reconstructed in the following way. Pairs of opposite-charge muons passing the level-2 selection ( $\mu 6\mu 3^2$ ) were fitted to a common vertex and their invariant mass calculated. The  $\chi^2/\text{d.o.f.}$  of the vertex fit was required to be less than 6.0, and the decay vertex of the  $J/\psi$  was required to be detached from the primary vertex by at least  $250\ \mu\text{m}$  in the transverse plane. The  $J/\psi$  mass resolution was found to be 39 MeV. The resolution of the  $J/\psi$  decay vertex in the transverse plane was  $64\ \mu\text{m}$  [7]. The efficiency of the reconstruction within a three-standard-deviation mass window was 79%. If a  $J/\psi$  was found, the analysis proceeded with  $\eta$ -reconstruction in the electromagnetic calorimeter. The  $\eta$  reconstruction is described in more detail in Ref. [10].

The ATLAS electromagnetic calorimeter (ECAL) is a LAr sampling calorimeter with three sampling layers [11]. The energy resolution is about  $\sigma(E)/E = 10\%/\sqrt{E} \oplus 1\%$  ( $E$  in GeV). The high-granular part of the ECAL extends up to  $|\eta| < 2.5$ , *i.e.* it has the same coverage as the Inner Detector. The basic cell is  $0.025$  in  $\Delta\eta$  and  $0.025$  in  $\Delta\phi$  in the second sampling layer. The clusterization algorithm uses a sliding window of  $3 \times 3$  cells and a cluster energy threshold of 1 GeV. A cluster is defined as the shower sampling inside a window of  $3 \times 5$  cells in the second ECAL layer.

In the simulated signal sample, in 20% of the  $\eta \rightarrow \gamma\gamma$  decays, the decay angle between the two photons is greater than  $5^\circ$ , the transverse energies of the photons are greater than 1 GeV, and both photons are within pseudorapidity range  $|\eta| < 2.5$ . In this case, two separate clusters could be reconstructed in the ECAL. An algorithm based on the selection of two highest transverse energy clusters was applied to reconstruct the  $\eta$ .

Clusters originating from hadrons, background photons and noise were suppressed by the following requirements:

- clusters were rejected if more than 4% of the total transverse energy was deposited in the third sampling of the ECAL or if more than 10% of the total transverse energy was deposited in the first sampling of the hadron calorimeter;
- clusters were rejected if the total cluster width, calculated by using the energy deposition in the 40 strips of the first sampling, was larger than 8 strips;
- clusters were required to have less than 20% of the energy deposited outside the  $3 \times 3$  window in both  $\eta$  and  $\phi$  direction within a larger

---

<sup>2</sup>In the following, the notation  $\mu 6$  ( $\mu 3$ ) is used to indicate a muon with a  $p_T > 6$  (3) GeV.

window of  $3 \times 7$ .

After the cuts, the obtained mass distribution was fitted with two Gaussians, with widths 35 MeV and 135 MeV. As can be seen from Fig. 1, the distribution of the background is asymmetric, and therefore the fitted mass values are shifted. The narrow Gaussian is shifted by 10 MeV, while the wider Gaussian describes essentially the background distribution. The  $\eta$ -reconstruction efficiency was 2.3% within two standard deviations ( $\pm 70$  MeV) of the nominal mass, and the background was 28%.

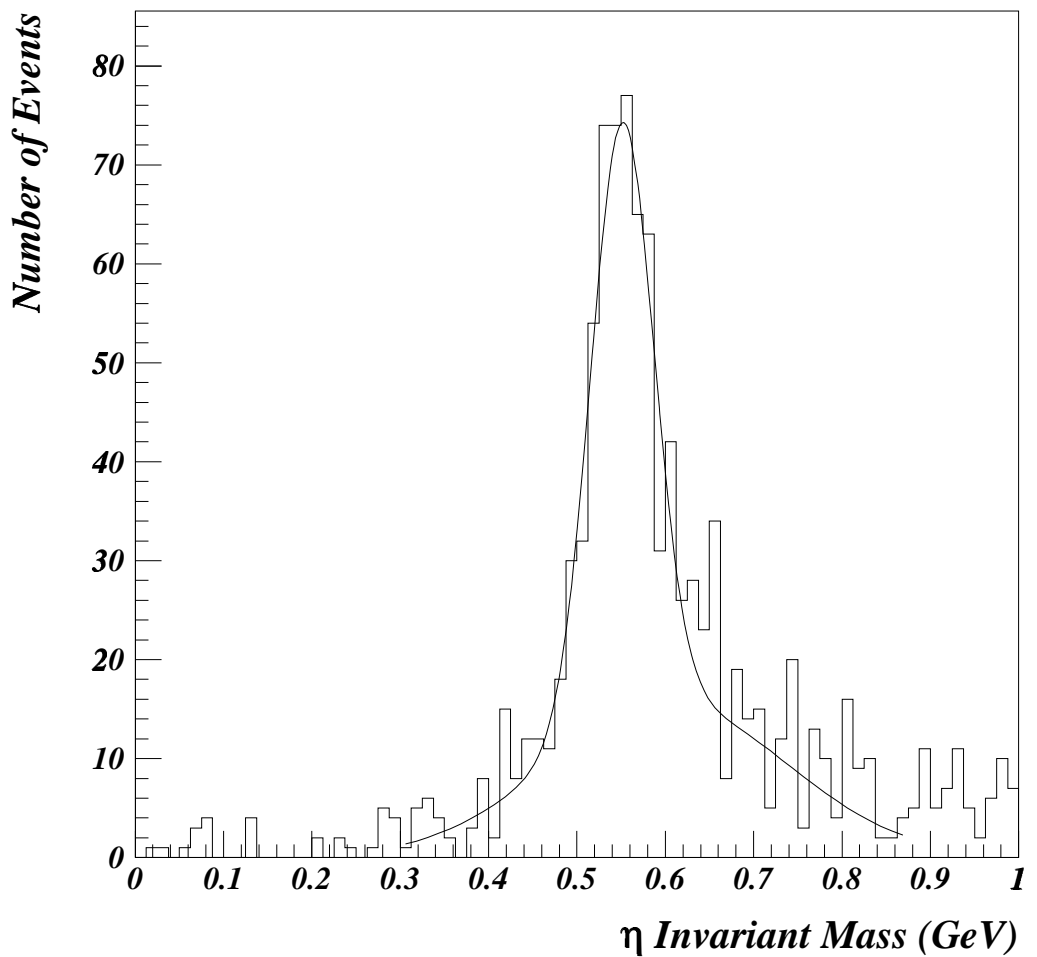


Figure 1: Invariant mass distribution of  $\eta$ -mesons in signal events after all the cuts.

A single-cluster selection was also tried, but the background turned out to be in this case much larger, 85%, than in the two-cluster case, so the

single-cluster events were not used. Photons which convert into  $e^+e^-$  pairs in the Inner Detector were reconstructed as well, but the statistical gain was found to be marginal.

The reconstructed  $J/\psi$  mesons within a three-standard-deviation mass window and the reconstructed  $\eta$  mesons within a two-standard-deviation mass window were then combined to form a  $B_s^0$  candidate. Their masses were constrained to the nominal values. Since the angular resolution of the calorimeter is not comparable with the tracker resolution, no further vertexing was performed. The obtained mass distribution was fitted with two Gaussians, with widths 67 MeV and 227 MeV, both centered at the nominal  $B_s^0$  mass. The relative fractions were 61% and 39%, respectively, within three standard deviations of the narrower Gaussian (the mass cut applied when selecting the signal events). The two Gaussians originate from the  $\eta$  mass distribution (see Fig. 1). The mass distribution of the reconstructed  $B_s^0$ -mesons is shown in Fig. 2.

The overall signal efficiency was found to be 1.1%, obtained by multiplying the  $J/\psi$  efficiency (79%), the muon efficiencies (85% and 78%), the  $\eta$  efficiency (2.3%), and requiring that the reconstructed  $B_s^0$  mass is within three standard deviations ( $\pm 201$  MeV) of the nominal mass. The background efficiency was  $\leq 0.009\%$ , obtained by multiplying the background reconstruction efficiency  $\leq 0.013\%$  with the muon reconstruction efficiencies. The study of the background rejection was limited by the statistics of the simulated background sample (23 000 inclusive  $b\bar{b} \rightarrow J/\psi X$  events). Out of this sample, no events remained in the  $B_s^0$  mass range after all the cuts, so it was assumed that the number of background events is less or equal to three at 95% CL, using Poisson limits [1].

The reconstruction of the decay  $B_d^0 \rightarrow J/\psi\eta$  was performed in an identical way. The obtained mass distribution was fitted with two Gaussians, with widths 67 MeV and 190 MeV, both centered at the nominal  $B_d^0$  mass. The relative fractions were 55% and 45%, respectively. The overall signal efficiency was found to be 1.0%. The background efficiency was  $\leq 0.009\%$ , since no events remained in the  $B_d^0$  mass range either after all the cuts. The mass distribution of the reconstructed  $B_d^0$ -mesons is shown in Fig. 3.



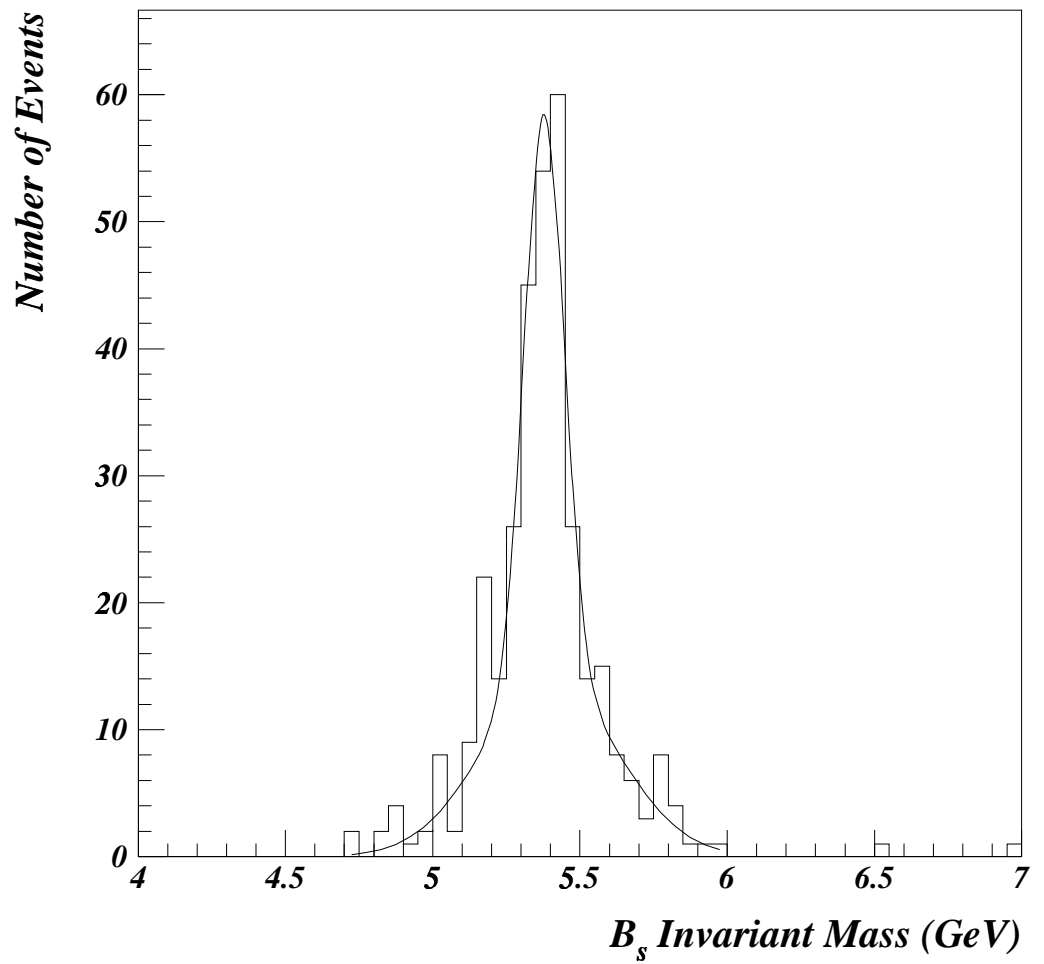


Figure 2: Invariant mass distribution of the reconstructed  $B_s^0$ -mesons in signal events after all the cuts apart from the final mass cut.

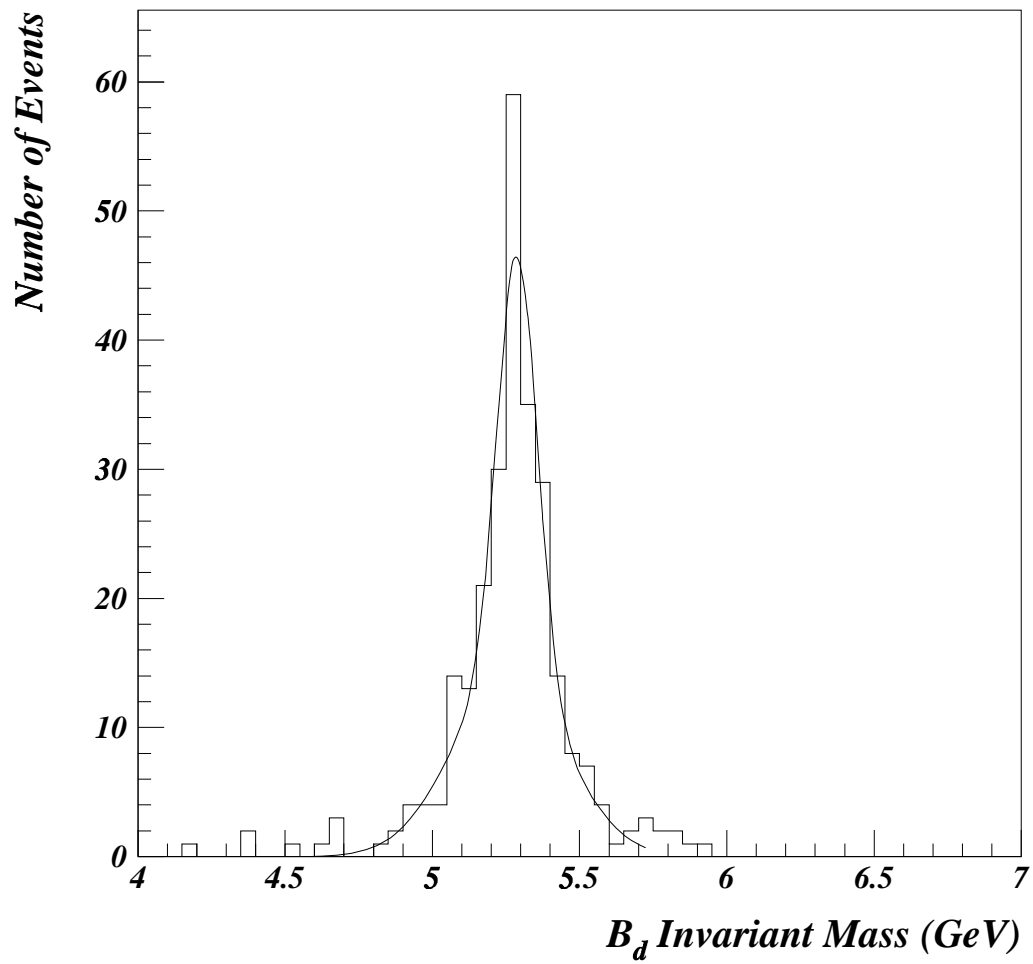


Figure 3: Invariant mass distribution of the reconstructed  $B_d^0$ -mesons in signal events after all the cuts apart from the final mass cut.

### 3 Results

#### 3.1 Event rates

The number of signal events, passing the ATLAS level-1 and level-2 triggers, was estimated as:

$$N_{\text{S}}^{\text{prod}} = 2\sigma(\text{pp} \rightarrow \text{b}\bar{\text{b}})\mathcal{B}\text{r}(\text{b} \rightarrow \text{B}_{\text{s,d}}^0)\mathcal{B}\text{r}(\text{B}_{\text{s,d}}^0 \rightarrow \text{J}/\psi\eta)\mathcal{B}\text{r}(\text{J}/\psi \rightarrow \mu^+\mu^-) \\ \cdot A(\mu 6)A(\mu 3)\mathcal{B}\text{r}(\eta \rightarrow \gamma\gamma) \int \mathcal{L}dt,$$

where  $A(\mu 6)$ ,  $A(\mu 3)$  are the kinematical acceptances for selecting a muon with  $p_{\text{T}} > 6(3)$  GeV,  $|\eta| < 2.4(2.5)$ .

Taking an integrated luminosity of  $30 \text{ fb}^{-1}$ , the  $\text{J}/\psi$  and  $\eta$  branching fractions from Ref. [1], and the production cross-section and the kinematical acceptances from the PYTHIA event generator, the number of produced  $\text{B}_{\text{s}}^0$  and  $\text{B}_{\text{d}}^0$  signal events was :

$$N_{\text{Bs}}^{\text{prod}} = 9.2 \cdot 10^8 \cdot \mathcal{B}\text{r}(\text{B}_{\text{s}}^0 \rightarrow \text{J}/\psi\eta), \\ N_{\text{Bd}}^{\text{prod}} = 4.9 \cdot 10^9 \cdot \mathcal{B}\text{r}(\text{B}_{\text{d}}^0 \rightarrow \text{J}/\psi\eta).$$

The number of observed events was:

$$N_{\text{Bs,Bd}}^{\text{obs}} = N_{\text{Bs,Bd}}^{\text{prod}} \cdot \epsilon(\text{B}_{\text{s,d}}^0)_{\text{rec}}.$$

The signal reconstruction efficiency was found to be 0.011 for the  $\text{B}_{\text{s}}^0$  and 0.010 for the  $\text{B}_{\text{d}}^0$ . The branching ratios calculated in Ref. [3], as well as the numbers of events, are given in Table 1. Using the branching ratios with  $\theta_{\text{P}} = -20^\circ$ , the number of observed signal events would be 9 600 and 80 for  $\text{B}_{\text{s}}^0$  and  $\text{B}_{\text{d}}^0$ , respectively. With  $\theta_{\text{P}} = -10^\circ$ , the numbers of observed signal events would be 8 400 and 200. In both cases, it is clear that the  $\text{B}_{\text{d}}^0$  signal cannot be observed. However, given the level of background (see later), it will be possible to set limits on the  $\text{B}_{\text{d}}^0$  branching fraction, based on the width and the central value of the reconstructed mass distribution. The accuracy of the limits will be given by the uncertainties in the mass reconstruction and efficiencies.

The number of background events was estimated as:

$$N_{\text{back}}^{\text{prod}} = \sigma(\text{pp} \rightarrow \text{b}\bar{\text{b}} \rightarrow \text{J}/\psi\text{X})A(\mu 6)A(\mu 3) \int \mathcal{L}dt.$$

Using the estimates obtained from PYTHIA, the number of produced background events was

$$N_{\text{back}}^{\text{prod}} = 1.2 \cdot 10^8.$$

	$\theta_P = -10^\circ$	$\theta_P = -20^\circ$
$\mathcal{B}r(\text{B}_s^0 \rightarrow \text{J}/\psi\eta)$	$8.3 \cdot 10^{-4}$	$9.5 \cdot 10^{-4}$
$N_{\text{B}_s}^{\text{obs}}$	8 400	9 600
$\mathcal{B}r(\text{B}_d^0 \rightarrow \text{J}/\psi\eta)$	$4.1 \cdot 10^{-6}$	$1.6 \cdot 10^{-6}$
$N_{\text{B}_d}^{\text{obs}}$	200	80
$N_{\text{back}}^{\text{obs}}$	10 800	10 800

Table 1: Estimated branching ratios for  $\text{B}_{s,d}^0 \rightarrow \text{J}/\psi\eta$ , and the numbers of signal and background events for an integrated luminosity of  $30 \text{ fb}^{-1}$ .  $\theta_P$  is the  $\eta - \eta'$  mixing angle, as estimated in Ref. [12].

Using  $\epsilon(\text{back})_{\text{rec}} = 0.009 \%$ , the number of observed background events was  $N_{\text{back}}^{\text{obs}} = 10800$ . A signal-to-background ratio of about 1:1 can be thus achieved for the  $\text{B}_s^0$  signal.

The mass distribution of the reconstructed  $\text{B}_s^0$ -mesons and the background is shown in Fig. 4.

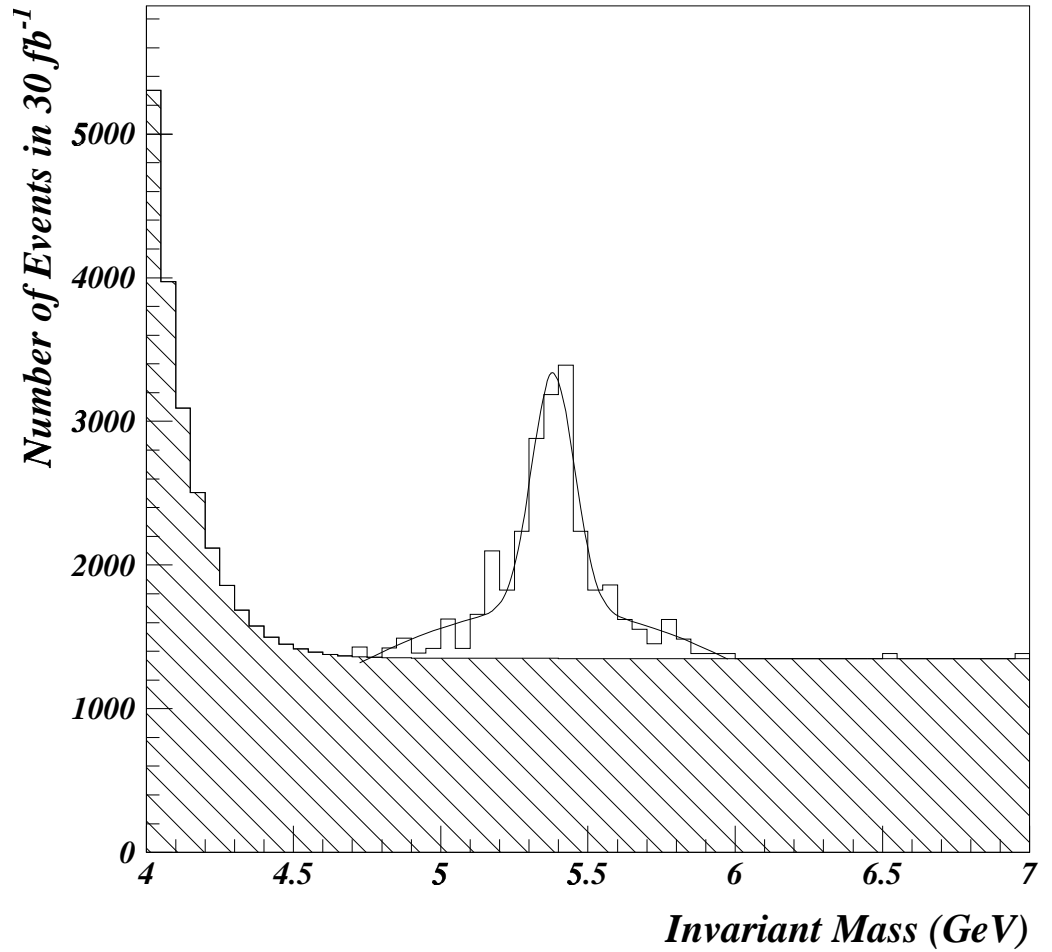


Figure 4: Invariant mass distribution of the reconstructed  $B_s^0$ -signal and background (white histogram) and the background (shaded histogram) after all the cuts apart from the final mass cut. The background mass distribution has been smoothed due to the insufficient simulation statistics.

### 3.2 Measurement of CP asymmetry

For the measurement of the CP asymmetry in the  $B_s^0$ -system, the events have to be tagged for distinguishing production of  $B_s^0$  and  $\bar{B}_s^0$ . In ATLAS, the tagging methods studied for tagging B-decays into  $J/\psi$ , where the  $J/\psi$  decays into two muons, are opposite-side lepton tagging, and same-side jet-charge tagging. The same-side jet-charge tagging exploits the correlation between the charge of a jet and the charge of the quark producing the jet. The B- $\pi$  correlation tagging, which is a special case of jet-charge tagging, is less effective for  $B_s^0$  because the mass of the  $B^{**}$  is expected to be such that the decay to  $B_s^0 K$  is not kinematically possible [13]. Opposite-side jet-charge tagging is difficult at hadron collider experiments, since additional b-jet tagging would be required to find the other b-jet.

The jet charge was defined as :

$$Q_{\text{jet}} = \frac{\sum_i q_i p_i^k}{\sum_i p_i^k},$$

where  $q_i$  is the charge of the  $i^{\text{th}}$  particle in the jet, and  $p_i$  is the momentum. All charged particles with  $p_T > 0.5$  GeV,  $|\eta| < 2.5$  around the reconstructed B-meson were included in the jet, if the distance between the particle and the B-meson,  $\Delta R = \sqrt{\eta^2 + \phi^2}$ , was less than 0.8. Particles not originating from near the primary vertex were excluded by requiring that the transverse impact parameter  $d_0$  was less than 1 cm and the  $z$ -coordinate of the particle at the point of closest approach was within 5 cm of the  $z$  of the primary vertex. The particles from the B-meson decay itself were excluded as well. In the analysis, the reconstructed B-meson was defined as  $B_s^0$  ( $\bar{B}_s^0$ ) if the jet-charge had  $Q_{\text{jet}} > +c$  ( $Q_{\text{jet}} < -c$ ), where  $c$  is a tunable cut.

The exponent  $k$  was optimized to maximize the tagging quality factor  $Q = D_{\text{tag}}^2 \cdot \epsilon_{\text{tag}}$ , where  $D_{\text{tag}}$  is the tagging dilution factor, originating from wrong-sign tags ( $D_{\text{tag}} = 1 - 2W$ , where  $W$  is the fraction of wrong-sign tags), and  $\epsilon_{\text{tag}}$  is the tagging efficiency. The optimum parameters were found to be  $k = 0.2$ ,  $c = 0.2$ , resulting in a quality factor of 3.85% with  $D_{\text{tag}} = 0.26$ ,  $\epsilon_{\text{tag}} = 0.57$ .

The quality factors of lepton tags were reported in Ref. [7] to be 0.25% for electron tags and 0.68% for muon tags. The study was performed for  $B_d^0 \rightarrow J/\psi(\mu\mu)K_S^0$  decays, so the event kinematics should be similar to the case considered here. Since the jet-charge tagging provided much better statistical power, the lepton tagging was not used here.

The observable asymmetry is :

$$a_{\text{obs}}(t) = Da_{CP}(t) = D \sin \phi_M \sin \Delta m_s t,$$

where  $D = D_{\text{tag}} D_{\text{back}}$  combines the experimental dilution factors due to mistagging and background.  $D_{\text{back}} = N_S^{\text{obs}} / (N_S^{\text{obs}} + N_{\text{back}}^{\text{obs}})$  is the ratio of the number of observed signal events to the total number of observed events.

Using the values  $\Delta\tau = 0.073$  ps for the decay time resolution [14],  $\tau_{B_s} = 1.464$  ps for the  $B_s$  lifetime [1],  $N_s^{\text{tag}} = \epsilon_{\text{tag}} N_s^{\text{obs}} = 0.57 \times 9600$  and  $N_{\text{back}}^{\text{tag}} = \epsilon_{\text{tag}} N_{\text{back}}^{\text{obs}} = 0.57 \times 10800$  (assuming that the tagging efficiency is the same for the background than for the signal), the error on the CP asymmetry was estimated to be:

$$\begin{aligned}\delta(\sin \phi_M) &= 0.27, \quad x_s = \Delta m_s / \Gamma_s = 19, \\ \delta(\sin \phi_M) &= 0.31, \quad x_s = 30,\end{aligned}$$

using a single-parameter fit. The  $x_s$  value of 19 represents the present experimental lower limit [1].

While the experimental resolution is not sensitive to a CP asymmetry of a few per cent, which is the case of the asymmetry predicted by the Standard Model, there could be some sensitivity to an asymmetry at the level of 40%, as predicted by some models beyond the Standard Model. The width difference of the  $B_s^0$  eigenstates was not taken into account in the analysis. ATLAS is expected to measure the width difference  $\delta(\Gamma_s)$  with a relative error of 12 %(stat.)  $\oplus$  7 %(syst.) (with  $\delta(\Gamma_s)/\Gamma_s = 0.15$ ) using the decays  $B_s^0 \rightarrow J/\psi\phi$  [7].

The measurement of the angle  $\gamma$  from the decay rates of  $B_s^0$  and  $B_d^0$  to  $J/\psi\eta$  is impossible because the decay  $B_d^0 \rightarrow J/\psi\eta$  cannot be observed.

## 4 Comparison to the other experiments

The PEP-II and KEKB B-factories cannot produce  $B_s^0$  mesons in the standard mode of running. It is foreseen that these B-factories could be run at the  $\Upsilon(5S)$  in order to be able to produce a sample of  $B_s^0$  mesons via  $\Upsilon(5S) \rightarrow B_s^{(*)} B_s^{(*)}$ , but whether this will be realized is highly uncertain, since running the accelerators at the  $\Upsilon(5S)$  will have much lower priority compared to the standard operation mode at the  $\Upsilon(4S)$  [15].

The hadron colliders Tevatron and LHC are the natural places to study  $B_s^0$  mesons. In ATLAS, the relative rate of reconstructed  $B_s^0 \rightarrow J/\psi\eta$  to  $B_s^0 \rightarrow J/\psi\phi$  is about 1:31 (300 000 reconstructed  $B_s^0 \rightarrow J/\psi\phi$  decays for  $30 \text{ fb}^{-1}$ ). In CDF, the estimated number of  $B_s^0 \rightarrow J/\psi\phi$  events in Run II (integrated luminosity  $2 \text{ fb}^{-1}$ ) is about 6 000 [16]. The CDF electromagnetic calorimeters are not more performant than the ATLAS ECAL. The central calorimeter is a lead-scintillator calorimeter with embedded strip chambers. The energy resolution is about  $\sigma(E)/E = 13.5\%/\sqrt{E \sin\theta} \oplus 1\%$  ( $E$  in GeV)[17]. The end-cap plug calorimeters for the Run II are lead-scintillator calorimeters with  $\sigma(E)/E = 16\%/\sqrt{E} \oplus 1\%$  ( $E$  in GeV) [18]. The pile-up should not deteriorate the performance at Tevatron. Assuming the same event ratio of  $B_s^0 \rightarrow J/\psi\eta$  to  $B_s^0 \rightarrow J/\psi\phi$  as for ATLAS, *i.e.* assuming the same reconstruction efficiency for  $\eta$  as in ATLAS, the signal sample of  $B_s^0 \rightarrow J/\psi\eta$  would be 190 events at CDF. The CDF estimate

given in Ref. [19] is larger than ours, apparently due to the fact that the only constraints for the  $\eta$  reconstruction in Ref. [19] were cuts on the photon transverse energy and pseudorapidity range. The number of signal events given for the BTeV experiment in the channel  $B_s^0 \rightarrow J/\psi\eta$ ,  $\eta \rightarrow \gamma\gamma$  was about 5 500 per year using the same branching fraction as in this paper.

The LHCb electromagnetic calorimeter is a lead-scintillator Shashlik-type calorimeter with a preshower detector, with a typical energy resolution of  $\sigma(E)/E = 10\%/\sqrt{E} \oplus 1.5\%$  ( $E$  in GeV) [20]. The resolution is thus similar to the ATLAS ECAL resolution. The great difference is the lever arm. The calorimeter is located at a distance of about 12.5 m from the interaction point. In the innermost section of the calorimeter, one calorimeter cell covers about 3 mrad. For comparison, a cell in the second sampling of the ATLAS ECAL covers about 25 mrad in  $\phi$  and 0.025 in  $\eta$  (about 25 mrad at  $\eta = 0$ , 16 mrad at  $\eta = 1$ ). The ability of the LHCb electromagnetic calorimeter to separate the two photon clusters from the  $\eta$  decay should thus be much better than in case of ATLAS. In LHCb, the estimated number of  $B_s^0 \rightarrow J/\psi\phi$  events in five years of operation ( $10 \text{ fb}^{-1}$ ) is about 370 000 [14]. We are not aware of any published results of the LHCb  $\eta$  reconstruction efficiency, while the  $\pi^0$  efficiency was found to be 25%, with a signal-to-background ratio of about 1:1 [21]. Assuming that the  $\eta$  reconstruction efficiency would be the same as the  $\pi^0$  reconstruction efficiency, the number of reconstructed  $B_s^0 \rightarrow J/\psi\eta$  events would be about 130 000. The number of reconstructed  $B_d^0$  decays would be about 1 075 with the same assumptions. The separation of the  $B_d^0$  signal from the  $B_s^0$  mass peak depends on the mass resolution and the background conditions, which are difficult for us to estimate.

These results should be taken as crude estimations, which were based on the publicly available information on the detector and accelerator performance.

## 5 Summary and outlook

The observation potential of the decays  $B_{s,d}^0 \rightarrow J/\psi\eta$  with the ATLAS detector at the LHC has been studied. At present there exist only upper limits for the branching fractions, but at LHC, a clear signal for the decay mode  $B_s^0 \rightarrow J/\psi\eta$ ,  $\eta \rightarrow \gamma\gamma$ , is expected. In ATLAS, 8 400 – 9 600 signal events are expected to be reconstructed with an integrated luminosity of  $30 \text{ fb}^{-1}$ , with a signal-to-background ratio of about 1:1. The branching fraction of this decay mode can thus be measured, and other parameters such as  $B_s^0$  lifetime can be measured as well.

For the decay  $B_d^0 \rightarrow J/\psi\eta$ , the expected signal consists of only 80 – 200 events, not visible above the background. With the ATLAS mass resolution of 67 MeV, the  $B_d^0$  signal cannot be separated from the  $B_s^0$  signal.



In the decay mode  $B_s^0 \rightarrow J/\psi\eta$ , the CP asymmetry predicted by the Standard Model is very small, a few per cent, and the observation of a sizeable effect would be a signal of physics beyond the Standard Model. The experimental resolution of the CP asymmetry was found to be 0.27 with  $x_s = 19$  and 0.33 with  $x_s = 30$ . There could thus be some sensitivity to very large asymmetries as predicted by some models beyond the Standard Model.

The ATLAS results are expected to be collected at the first years of the LHC operation, running at the low luminosity  $((1 - 2) \cdot 10^{33} \text{cm}^{-2}\text{s}^{-1})$ . The LHCb experiment will eventually be able to collect more statistics, since the forward spectrometer geometry with a long lever arm is more favourable for  $\eta \rightarrow \gamma\gamma$  reconstruction. During five years of LHC operation, the LHCb is expected to collect an integrated luminosity of  $10 \text{fb}^{-1}$ , giving about 130 000 signal events in the  $B_s^0$  channel according to our estimates. The combined potential of the LHC experiments is thus very promising.

## 6 Acknowledgements

This work has been performed within the ATLAS Collaboration, and we thank collaboration members for helpful discussions. We have made use of the physics analysis framework and tools which are the result of collaboration-wide efforts. P.E. would like to thank the hospitality of ISN Grenoble and the support from the French Ministry of Education for making it possible to visit Grenoble and finalize this work.

## References

- [1] D.E. Groom *et al.*, Eur. Phys. J. C15 (2000) 1 and 2001 off-year partial update for the 2002 edition, available on the PDG WWW pages (URL: <http://pdg.lbl.gov/>).
- [2] M. Acciarri *et al.*, L3 Collaboration, Phys. Lett. B 391 (1997) 481.
- [3] P.Z. Skands, JHEP 1 (2001) 8.
- [4] A. Ali and D. London, Eur. Phys. J. C9 (1999) 687.
- [5] P. Ball and R. Fleischer, Phys. Lett. B475 (2000) 111.
- [6] T. Sjöstrand, Computer Physics Commun. 82 (1994) 74.
- [7] ATLAS Collaboration, ATLAS Detector and Physics Performance Technical Design Report Vol II, CERN/LHCC/99-15 (1999).
- [8] ATLAS Collaboration, ATLAS Detector and Physics Performance Technical Design Report Vol I, CERN/LHCC/99-14 (1999).
- [9] S. Simion, 'Pile-up Simulation for Atlas Calorimeters', ATLAS Internal Note ATL-SOFT-99-001 (1999).
- [10] F. Ohlsson-Malek and M. Melcher, 'ATLAS calorimeter performance for identification of  $\gamma$ ,  $\pi^0$  and  $\eta$  particles at low transverse momentum', ISN-01.75 and ATLAS Internal Note ATL-COM-PHYS-2001-021 (2001).
- [11] ATLAS Collaboration, ATLAS Calorimeter Performance Technical Design Report, CERN/LHCC/96-40 (1996).
- [12] T. Feldman, Int. J. Mod. Phys. A15 (2000) 159.
- [13] E.J. Eichten, C.H. Hill and C. Quigg, Phys. Rev. Lett. 71 (1993) 4116; E.J. Eichten, C.H. Hill and C. Quigg, 'Orbitally Excited Heavy-Light Mesons Revisited', FERMILAB-CONF-94/118-T (1994).
- [14] P. Ball *et al.*, 'B Decays at the LHC', CERN-TH/2000-101, hep-ph/0003238 (March 2000).
- [15] See *e.g.* The BaBar Physics Book, BaBar Collaboration (P.F. Harrison, ed. *et al.*) SLAC-R-504 (1998).
- [16] V. Papadimitriou, Nucl. Instrum. and Methods A446 (2000) 143.
- [17] L. Balka *et al.*, Nucl.Instrum. and Methods A267 (1988) 272.

- [18] See *e.g.* The CDF II Detector Technical Design Report in <http://www-cdf.fnal.gov/upgrades/tdr/tdr.html>.
- [19] K. Anikeev *et al.*, 'B Physics at the Tevatron: Run II and Beyond', FERMILAB-Pub-01/197, hep-ph/0201071 (December 2001).
- [20] LHCb Calorimeters Technical Design Report, CERN-LHCC/2000-0036 (2000).
- [21] A. Jacholkowska, Nucl. Instrum. and Methods A446 (2000) 259.